Flash flooding prediction in regions of northern Vietnam using the KINEROS2 model

Hong Quang Nguyen, Jan Degener and Martin Kappas

ABSTRACT

Flash flooding (FF) in Vietnam has become an important issue due to increasing loss of property and life. This paper investigates FF prediction using the Kinematic Run-off and Erosion model to perform comprehensive analyses to: (1) evaluate the role of initial soil moisture (θ) conditions using the Bridging Event and Continuous Hydrological model; (2) model the discharge (Q) using different rainfall inputs; (3) test the sensitivities of the model to θ and Manning's n coefficient (N) on Q and validate the model; and (4) predict channel discharge (Q_C) using forecasted rainfall. A relative saturation index (R) of 0.46 and N of 0.14 produced the best match of the simulated outflow to measured Q, while the saturated hydraulic conductivity (Ksat) and R had significant effects on the magnitude of flooding. The parameter N had remarkable influences on the volume of flow and its peak time. Surprisingly, the use of radar rainfall data underestimated Q compared to the measured discharge and estimates using satellite rainfall. We conclude that the KINEROS2 model is well equipped to predict FF events in the study area and is therefore suitable as an early warning system when combined with weather forecasts. However, uncertainties grow when the forecasted period expands further into the future.

Key words | channel discharge, flash flood prediction, KINEROS2, satellite rainfall, tropics, Yen Bai

Hong Quang Nguyen (corresponding author)
Jan Degener
Martin Kappas
Department of Cartography, GIS and Remote
    Sensing,
Georg-August-University of Göttingen,
Goldschmidtstr. 5,
37077 Göttingen,
Germany
E-mail: hongquang116@yahoo.com

INTRODUCTION

Recently, there has been a growing interest in the damage caused by natural hazards (Creutin *et al.* 2013; Kousky & Walls 2014) and flash floods (FFs). The most devastating floods often cause heavy loss of life (Gupta 2006; Ashley & Ashley 2008; Brauer *et al.* 2011). In northern Vietnam, the development of FFs has induced an imperative need to mitigate their impact (NCHMF 2011). Despite this need, few attempts have been made to mitigate floods in the region. This lack of flood mitigation might be explained by the complexity of FFs themselves and by the remaining prevailing uncertainties (Montz & Gruntfest 2002; Estupina-Borrell *et al.* 2006; Ntelekos *et al.* 2006). An extensive amount of research has been accumulated worldwide on many aspects of FFs (Montz & Gruntfest 2002; Morin *et al.* 2009); many of these works suggested that a feasible approach to FF mitigation is to identify their occurrences early (Khavich & Benzvi 1995; Alfieri *et al.* 2012; Looper &

Vieux 2012; Quintero *et al.* 2012; Versini 2012). We used a modelling method employing the Kinematic Run-off and Erosion Model (KINEROS2) to assess a past FF on 23rd June 2011 (R23[rd]), the Bridging Event and Continuous Hydrological (BEACH) model to calculate θ as input to the KINEROS2, and the results from some meteorological models, namely the Global Spectral Model (GSM) (Krishnamurti *et al.* 2006) and the High Resolution Model (HRM) (Majewski 2009), for the forecast stage.

In 11 years, from 1995 to 2005, Vietnam experienced up to 300 FF events that resulted in the following losses: 968 people died, 628 people were injured, and material losses worth €71 million occurred. Most of the FFs were in the north of Vietnam (NCHMF 2011). The north of Vietnam, in general, and Yen Bai province, in particular, are identified as being very prone to FFs, and the people are highly exposed to FF problems. In Yen Bai province (case study

area), the R23rd event took four lives in the Nam Khat catchment area. FFs have not only resulted in loss of life and property but also negatively impacted society or had severe social consequences (Ruin *et al.* 2008). It is believed that for an advanced understanding of FFs, multidisciplinary approaches must be integrated (Villarini *et al.* 2010). This study focuses on the physical techniques of modelling FFs and their forecast prospects.

FF modelling is complex and linked to the problem of uncertainties (Beven 2001). Although there are large numbers of studies on FFs, their behaviours are not fully understood (Sahoo *et al.* 2006). Many questions have been addressed, such as questions on the accuracy of model inputs and outputs (Li *et al.* 2010, 2013; Li & Xu 2014), model structure (Bloschl *et al.* 2008; Garcia-Pintado *et al.* 2009; Looper & Vieux 2012), initial conditions and boundary conditions (Abderrezzak *et al.* 2009; Vincendon *et al.* 2009; Seo *et al.* 2012), temporal and spatial scales (Amengual *et al.* 2007; Reed *et al.* 2007; Younis *et al.* 2008), and threshold-runoff uncertainties (Gupta 2006; Ntelekos *et al.* 2006). El-Hames & Richards (1998) suggested that, for a successful application of flood prediction, complex and comprehensive techniques are often required. Furthermore, as FFs occur shortly after the onset of rainfall events, hydrological models used for FF forecast must have the ability to evaluate the level of risk in a short time (Janal & Stary 2012).

We used the robust model of KINEROS2 for estimating and predicting Q$_C$ (a complete study framework is presented in the Materials and methods section). The model has already proven to be reliable for such tasks in semi-arid regions (Volkmann *et al.* 2010). The goal of our study is to evaluate its merits for a more humid sub-tropical environment, to identify the key variables that determine its output, and to assess its suitability to predict FF events based on different precipitation input data.

STUDY SITE

This study focuses on regions in northern Vietnam featuring similar climatic and morphological conditions of typical tropical, steep and dense drainage-network systems. Some representative watersheds in Yen Bai province were chosen for the actual modelling implementations.

The Nam Kim watershed, shown in Figure 1, was chosen for the KINEROS2 model validations using observed data records at its outlet. BEACH daily actual evapotranspiration (ETa) was computed for the three watersheds and compared with the Soil and Water Assessment Tool (SWAT) ETa. Nam Khat experienced the FF event on 23rd June 2011, which resulted in the loss of life and property. Many areas in Yen Bai province are prone to FF due to their conditions of annual precipitation of approximately 1,500 mm, average slopes of 28 degrees and a reduction of vegetation cover. The watersheds are located at approximately 1,200 meters a.s.l., where most residents belong to an ethnic minority and are potentially exposed to flooding. Ngoi Hut is the largest watershed and was used for testing the application of the KINEROS2 model for a larger watershed.

MATERIALS AND METHODS

Study flow chart

Figure 2 provides an overview of the steps to achieve the study objective of FF forecast. Model input preparations, calibrations, validations and connections are presented step-by-step in the following sections.

Channel routine equation

The basic equations of the channel routine were defined comprehensively in Woolhiser *et al.* (1990) and Smith *et al.* (1995) or, for the more recent version, KINEROS2 in Semmens *et al.* (2008). We only present the following kinematic channel equation solved by a four point implicit techniques (Woolhiser *et al.* 1990).

$$A_{j+1}^{i+1} - A_{j+1}^i + A_j^{i+1} - A_j^i + \frac{2\Delta t}{\Delta x}\left\{\theta_w\left[d\frac{Q^{i+1}}{dA}\left(A_{j+1}^{i+1} - A_j^{i+1}\right)\right]\right.$$
$$\left. +(1-\theta_w)\left[\frac{dQ^i}{dA}\left(A_{j+1}^i - A_j^i\right)\right]\right\}$$
$$= 0.5\Delta t\left(q_{cj+1}^{i+1} + q_{cj}^{i+1} + q_{cj+1}^i + q_{cj}^i\right) \tag{1}$$

where A is the cross-sectional area, q_c is the lateral inflow, θ_w is a weighting parameter (often 0.6 to 0.8) for the x
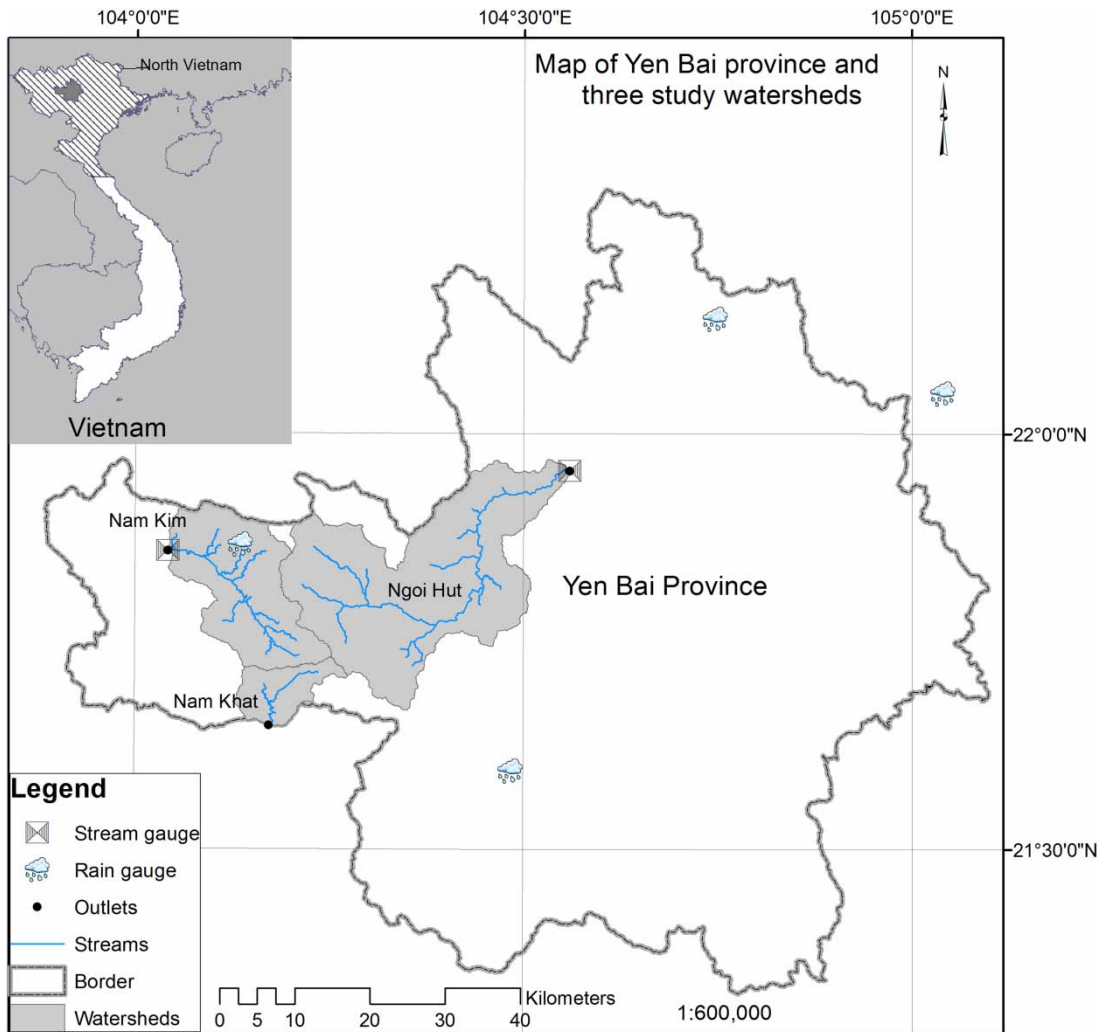
Figure 1 │ Study area of Nam Kim, Ngoi Hut and Nam Khat watersheds in Yen Bai province, Vietnam.

derivatives at the advanced time step (Δt), and Q is the discharge per unit width (L^{-2} T^{-2}); Newton's iteration technique is used to solve for the unknown area $\left[A_{j+1}^{i+1} \right]$.

The BEACH and SWAT models

Because the event-based KINEROS2 model does not compute inter-storm θ conditions, the antecedent θ (θ_{ant}) must be provided as the initial condition at the beginning of the model run. The daily soil moisture calculated by the BEACH model could be a good solution.

BEACH was developed by Sheikh *et al.* (2009) and is a spatially distributed daily basic hydrological model. The main aim of the model is to estimate the daily θ. More details about the model are referenced in Sheikh *et al.* (2009).

SWAT is a well-known hydrological distributed model. Details about the model and its applications can be found in Neitsch *et al.* (2009) and others. As the ETa is extremely difficult to validate, we used the SWAT ETa for calibrating the BEACH model.

Soil, land use/land cover and DEM

The land use/land cover (LULC) of Yen Bai province was mapped using Landsat 5 TM scenes (30×30-meter resolution) acquired in 2009. The map consists of six classes,
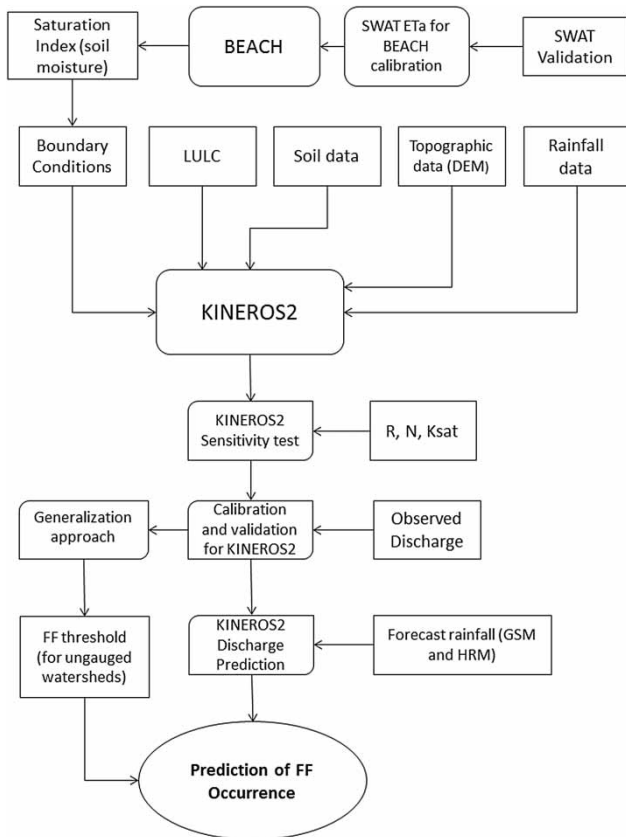
Figure 2 | Methodological flow chart of FF prediction.

including forest, shrub, agricultural land, grassland, water bodies and bare land. The soils of the regions are categorized into six major soil groupings: fluvisols, calcisols, ferralsols, alisols, acrisols and gleysols. The soils were derived from a custom soil map produced by the Environment and Resource Centre-Agricultural Institute of Plan and Design, Vietnam. The Digital Elevation Model (DEM) used for geomorphological inputs was provided by the Vietnam Resources and Environment Corporation and produced in 2009 using the Aerial Photogrammetric technology of the Intergraph Corporation, USA.

Rainfall data

We used several rainfall sources for this research including satellite-based (Sat-P), radar rainfalls (Rad-P), gauged and forecasted rainfall (FR). All the data were provided by the Vietnamese National Centre for Hydrological Forecasting.

The Sat-P of the R23[rd] event and the rainfall event on 30th June 2011 (R30[th]) was derived from 70 images. We developed a model (called SATAS) using the Model Builder application running within the ArcMap environment. The model extracts the rainfall from the original images.

Radar precipitation was derived from the data of two ground radar stations at Viet Tri and Phu Lien for the R23[rd] event and processed similarly together with the Sat-P using the SATAS. The spatial resolution of a radar scan was 2 kilometres, and the scanning-time interval was 5 minutes. The Rad-P was estimated using the conventional method of Marshall *et al.* (1947), as in the following relation:

$$z = 200R^{1.6} \tag{2}$$

where R (mm h^{-1}) is the rain rate, and z is the radar reflectivity factor.

Daily gauged-3-hour rainfall (Gau-P) was recorded by the rain gauge in Nam Kim (Figure 1) and extracted for the KINEROS2 validation of the rainfall on 8th (R8[th]) and 31st (R31[st]) July 2011. These data were accumulated to daily values and used as input for the SWAT model.

As the forecasted rainfall is a prerequisite for the FF prediction, we used the FR from the numerical weather prediction (NWP) of GSM (3.5 day forecast) and of HRM (5.5 day forecast). The GSM and HRM are operated in local watersheds at times of 00:00, 06:00, 12:00 and 18:00 and at times of 00:00 and 12:00, respectively. The Thiessen approach (Thiessen 1911) can be applied for generating distributed forecasting precipitation.

Stream gauged discharge

The *in situ* measured Q (daily and hourly) recorded by the stream gauges (Figure 1) was available for Nam Kim and Ngoi Hut. The daily data were used for the SWAT, and the hourly data were used for the KINEROS2 model.

SWAT calibration and validation

The model was calibrated over the five years from 2001 to 2005 for Nam Kim and Ngoi Hut. Some sensitive parameters were adjusted, as summarized in Table 1. Note

Table 1 | Top ten SWAT sensitive parameter and final values

Sensitivity order	Parameter	Description	Unit	Range	Initial value	Final value
1	CN2	Curve number condition 2	–	35–98	35	54.1
2	Alpha_Bf	Baseflow recession constant	days	0–1	0.04	0.4
3	Ch_K2	Effective hydraulic conductivity in channel	mm hr^{-1}	−0.01–500	50	75
4	Sol_K	Saturated hydraulic conductivity	mm hr^{-1}	0–2,000	2	4.30
5	Ch_N2	Manning n value for the main channel	–	−0.01–0.3	0.015	0.05
6	Surlag	Surface runoff lag coefficient	–	1–24	4	2.5
7	Sol_Awc	Available water capacity	mm mm^{-1}	0–1	0.22	0.31
8	Gw_Revap	Revap coefficient	–	0.02–0.2	0.02	0.2
9	Esco	Soil evaporation compensation factor	–	0-1	0	0.95
10	Gwqmin	Threshold water level in shallow aquifer for base flow	mm	0–5,000	0	0.50

that some final values were averaged from the values of hydrologic response units (HRUs). Model validation was applied after every calibration from 2006 to 2012. The goodness of agreement between the simulated data and the observed data were evaluated using the coefficient of determination (R^2), the Nash–Sutcliffe simulation efficiency coefficient (NSE) and graphical methods. These methods were also applied for BEACH and KINEROS2.

BEACH calibration

The BEACH calibrated parameters are represented in Table 2, based on the results of the calibration and validation of SWAT. As the BEACH estimates ETa for different types of crops, the SWAT ETa was calculated for each HRU representing the corresponding crop class for these comparisons.

KINEROS2 calibration and validation

The KINEROS2 model was calibrated for the R23rd event using the hourly gauged Q and Sat-P. Some significant changes of parameters were implemented in the calibration stage to make the model an acceptable simulator of the real hydrological system. These parameters are summarized in Table 3. Afterwards, the model validation was performed for the R30th (using Sat-P), R8th and R31st (employing Gau-P) events.

RESULTS

Results of SWAT calibration and validation

Compared to the daily observed data, significant overestimates of Q for Nam Kim and underestimates for Ngoi Hut exist before the calibration of the models (NSE ≈ −0.35) (Figure 3(a) and 3(c)). In contrast, the simulated discharge after calibration and validation matched closely to the measured data in both watersheds, with average R^2 of 0.79 and NSE of 0.65.

Results of KINEROS2 calibration and validation

In the first model run using the default parameters, θ of 46% and channel Manning's n coefficient (Nc) of 0.035, KINEROS2 simulated the Q as being much higher than in the observed data, and its peak was nearly double the gauged peak. The gap was reduced after the calibration stage, mostly due to increases in N and reductions in Ksat. This trend remained in the validations. The goodness of agreement is graphically depicted in Figure 4, with a mean R^2 of 0.93. The best correlation between simulated and observed Q was found for the R23rd event, and less agreement was found for the R31st event.

Comparing SWAT and BEACH ETa

Figure 5 indicates the positive correlation between evapotranspiration of the two models calculated for the

Table 2 | BEACH input variables and parameters

Variables	Notation	Unit	Grass	Shrub	Industrial plants	Rice	Thin forest	Forest
Curve number condition 2	CN_2	–	80	60	65	75	50	45
Initial basal crop coefficient	$K_{cb\ ini}$	–	0.03	0.20	0.17	0.15	0.30	0.40
Median basal crop coefficient	$K_{cb\ mid}$	–	0.30	0.80	1.10	0.85	1.20	1.50
End basal crop coefficient	$K_{cb\ end}$	–	0.15	0.25	0.25	0.85	0.85	0.70
Light use efficiency	μ	–	0.25	0.50	0.45	0.30	0.60	0.75
Maximum crop height	H_{max}	m	0.30	1.10	1.10	0.40	2.50	10.0
Maximum leaf area index	LAI_{max}	$m^2\ m^{-2}$	0.06	2.00	3.20	1.50	5.00	6.0
Maximum root depth	RD_{max}	m	0.30	1.70	1.50	0.50	1.70	2.50
Saturated hydraulic conductivity in surface layer	$K_{sat\ 1}$	$m\ d^{-1}$	0.06	0.10	0.10	0.09	0.10	0.11
Saturated hydraulic conductivity in second layer	$K_{sat\ 2}$	$m\ d^{-1}$	0.26	0.26	0.26	0.26	0.31	0.36
Soil evaporation depth	D_e	m	0.15	0.15	0.15	0.15	0.15	0.15
Soil moisture at saturation in surface layer	θ_1	$m^3\ m^{-3}$	0.45	0.50	0.55	0.55	0.55	0.60
Soil moisture at saturation in second layer	θ_2	$m^3\ m^{-3}$	0.50	0.60	0.65	0.55	0.65	0.70
Soil moisture at field capacity in surface layer	$\theta_{fc\ 1}$	$m^3\ m^{-3}$	0.15	0.23	0.20	0.25	0.30	0.40
Soil moisture at field capacity in second layer	$\theta_{fc\ 2}$	$m^3\ m^{-3}$	0.20	0.25	0.22	0.27	0.35	0.45
Soil moisture at wilting point	θ_{wp}	$m^3\ m^{-3}$	0.11	0.13	0.13	0.12	0.14	0.15
Subsurface flow coefficient	C	d^{-1}	0.25	0.25	0.25	0.25	0.25	0.25
Water stress sensitivity	p	–	0.55	0.55	0.55	0.45	0.75	0.85

**Table 3** | KINEROS2 parameter calibrated for the R23[rd] event

Parameter	Description	Unit	Range Plane	Range Channel	Initial value Plane	Initial value Channel	Optimal value[a] Plane	Optimal value[a] Channel
ksat	Saturated hydraulic conductivity	$mm\ h^{-1}$	0–10	20–50	3.7	41.7	4.46	45.5
s	Initial saturation	–	0–0.9	0–0.9	0.2	0.45	0.46	0.85
n	Manning's coefficient	–	0.01–1	0.01–1	0.035	0.036	0.07	0.14
ϕ	Soil porosity	–	–	–	0.1	0.44	0.47	0.44
g	Capillary length scale	mm	0-500	0-500	0	0	367.13	101
w	Woolhiser coefficient (channel microtopography)	–	NA	–	NA	0.15	NA	0.15
i	Interception depth	mm	–	–	2	NA	1.51	NA
p	Plant cover	–	–	NA	1	NA	0.52	NA
slp	Slope factor	–	0.5–1	NA	1	NA	0.66	NA
spl	Splash coefficient	$s\ m^{-1}$	25–150	NA	25	NA	121.37	NA

[a]Averaged values; NA = not applicable.

watersheds in 2011, with a NSE of 0.6 for both Nam Kim and Ngoi Hut watersheds and 0.62 for the Nam Khat watershed. The differences were greater from mid-January to mid-March. In all cases, the ETa peaked at approximately 25th March at above 10 mm d^{-1}. From May to November, the ET_a varied by approximately 2 mm d^{-1}. Correlations between the daily rainfall and evapotranspiration were also observed. On rainy days, the ETa
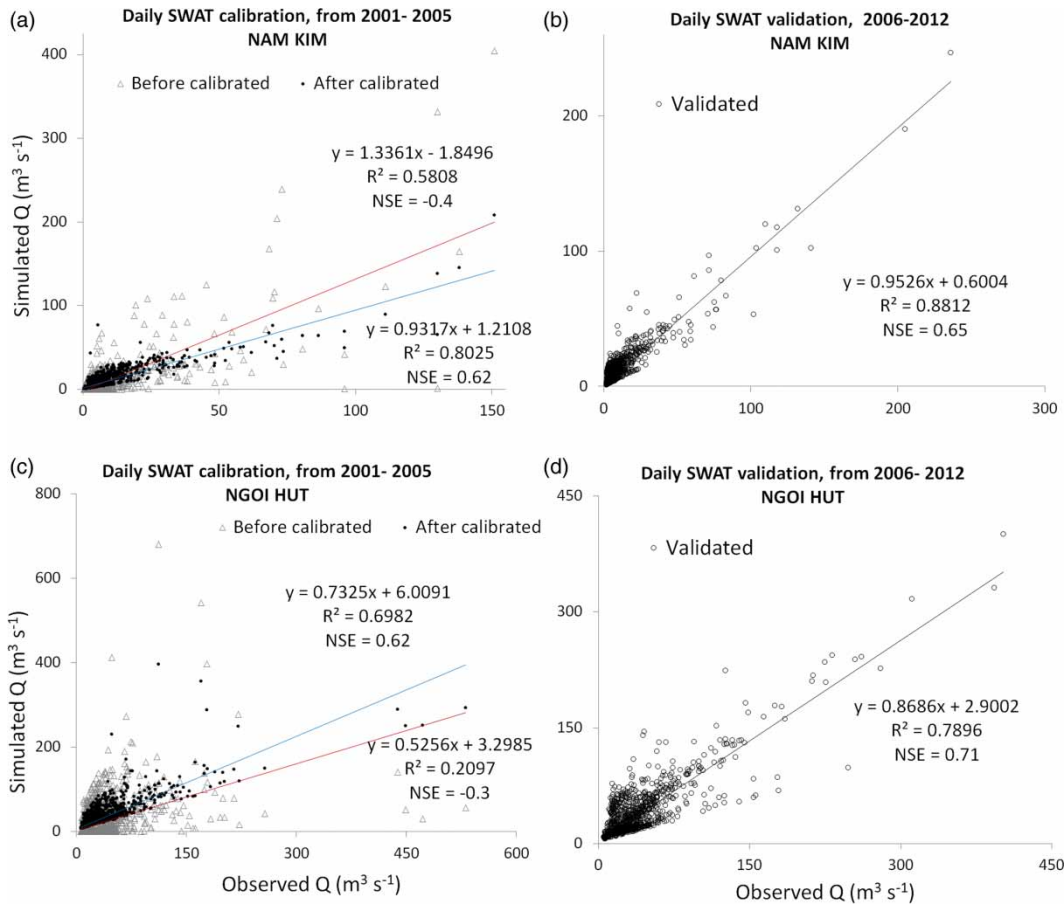
Figure 3 | Comparison between the gauged and the SWAT discharge in the Nam Kim and Ngoi Hut watersheds.

values were low; however, on the subsequent dry days, they rose sharply.

BEACH soil moisture

Figure 6 illustrates that the forest land was the wettest land, in contrast to the plant industrial zone. The differences between θ of forest land and the mean values (calculated considering area-weightings) were minimal because of the dominance of the forest area in Nam Kim. In both watersheds, from January to 20th March, the soil was the driest. In contrast, from May to October, the soil was wet, with the conditions gradually becoming drier. The mean θ on 22nd June 2011 was marked at 46% for the Nam Kim watershed and at 42% for the Nam Khat watershed and was used for the KINEROS2 modelled R23rd event.

Results of the KINEROS2 model

Model parameter sensitivity tests

The graphs (Figure 7(a) and 7(c)) show the impacts of changing θ_{ant} conditions on the estimated KINEROS2 outflow through the watershed outlets. The reduction of θ_{ant} from 50 to 20% resulted in declines of the peaks from 845 to 535 m^3 s^{-1} in the Nam Kim watershed and from 355 to 279 m^3 s^{-1} in the Nam Khat watershed. However, the reduction had no impact on the time to peak. In addition, the graphs (Figure 7(b) and 7(d)) presented the changes of both Q values and the time to peak while the Nc values were increased and θ_{ant} was kept unchanged. The peaks and the lags in Nam Kim (268 km^2) reduced sharply while the Nc was decreased. However, less sensitivity was found for Nam Khat

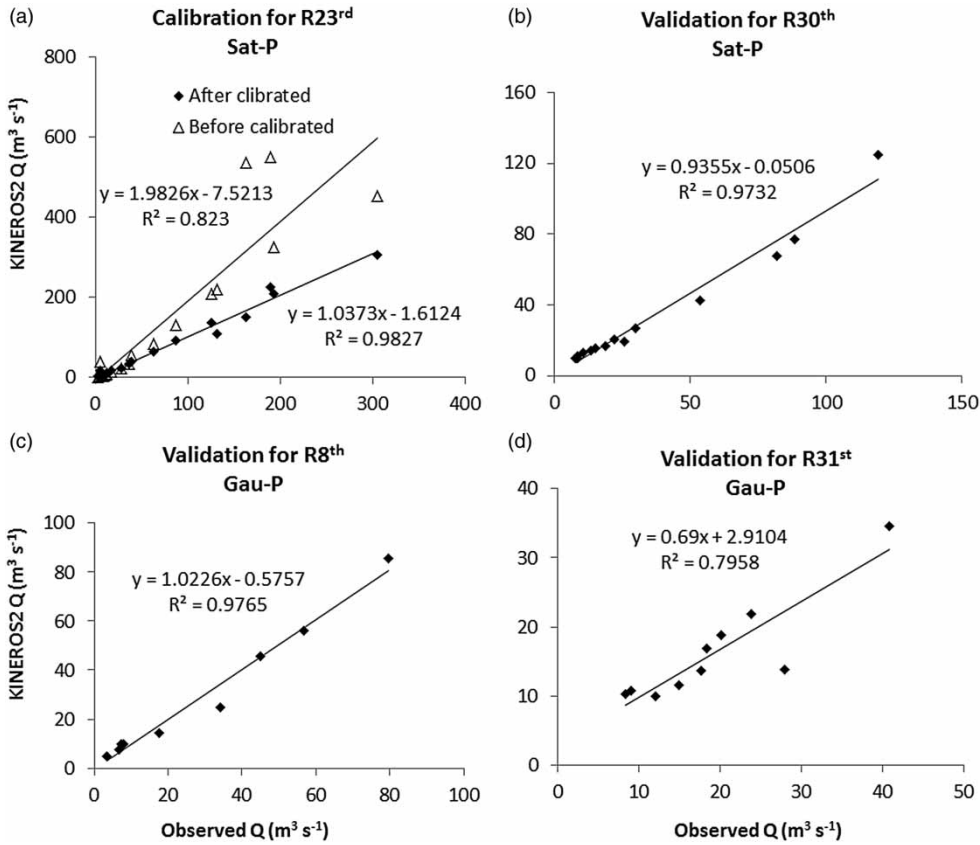**Figure 4** │ Scatter plots of the KINEROS2 calibration and validation for the R23[rd], R30[th], R8[th] and R31[st] events.
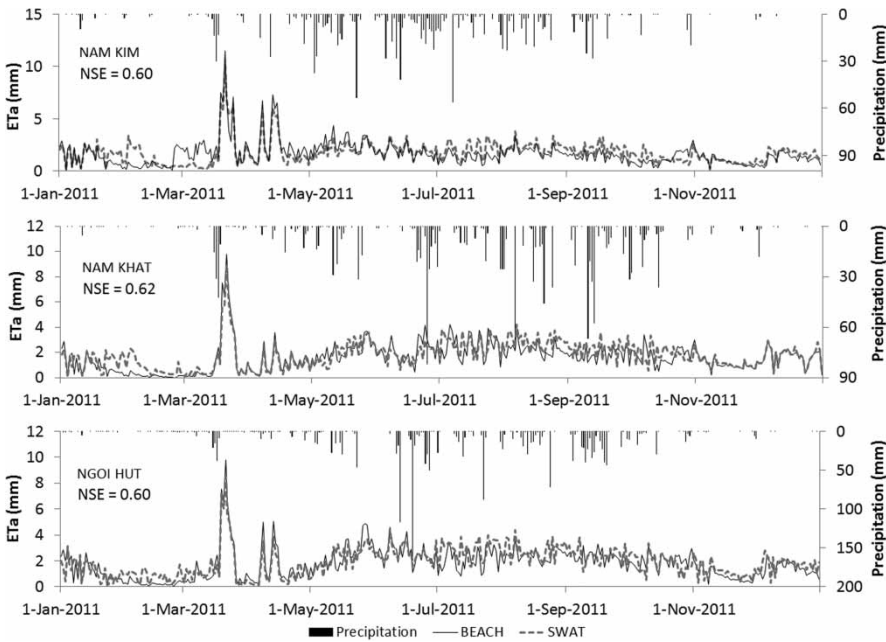

Figure 5 │ Comparison of the mean ETa values of the BEACH and SWAT simulations for the Nam Kim, Nam Khat and Ngoi Hut watersheds.
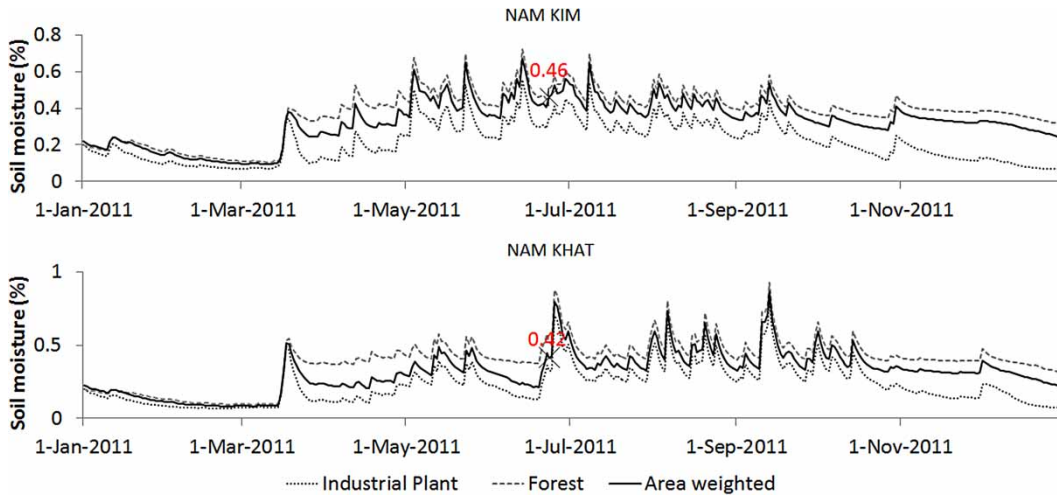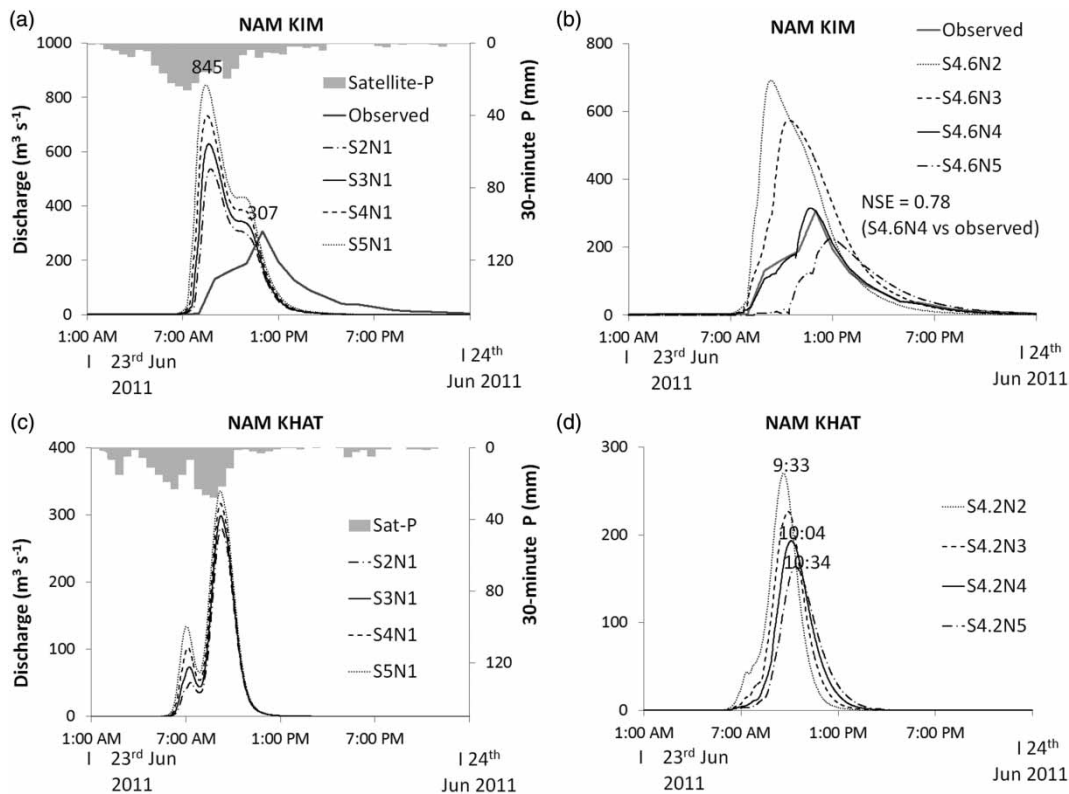
Figure 6 │ Daily BEACH soil moisture.

Figure 7 │ Effects of antecedent soil moisture and N on discharges (P denotes precipitation. S2, S3, S4, S5, S4.6 and S4.2 represent soil moisture conditions at 20%, 30%, 40%, 50%, 46% and 42%, respectively; N1, N2, N3, N4 and N5 indicate Manning's n roughness coefficients of 0.035, 0.07, 0.10, 0.140 and 0.175, respectively).

(74 km^2), with Q declines of 60 m^3 s^{-1} and lags of 30 minutes. The model predicted the Q fitting best to the observed flow at the θ conditions of 46% and the Nc of 0.14 (Figure 7(b), S4.6N4).

Ksat sensitivity test

The Ksat represents the most sensitive parameter of KINEROS2: with an increase or decrease of just 20% from

the initial values (see Table 3), great changes in simulated Q are found in the graphs compared to the results of the initial input (the continuous lines in the middle in Figure 8). However, the plane Ksat was more sensitive than the channel Ksat. In addition, the size of the watershed played a remarkable role in the impact of the Ksat, as depicted by the 'plump' graph of Nam Kim and the 'slender' one of Nam Khat.

Comparing discharge using Sat-P and Rad-P

While other inputs, such as θ and N, were kept unchanged, in general, using Rad-P produced lower peaks than using the Sat-P (≈observed) in both of the watersheds (Table 4). Although the total Sat-P and Rad-P rainfalls were not much different, the estimated time to peak of the Rad-P was 0.73 hours later than that using Sat-P in Nam Kim and 0.26 hours later than that in Nam Khat.

KINEROS2 stream discharges

The Nam Kim and Nam Khat watersheds were modelled using KINEROS2 and Sat-P, with an Nc of 0.14 and an S of 0.46 and 0.42, respectively. The peak flows of the streams and planes

are presented in Figure 9. Obviously, the flow volumes were positively proportional to the areas of the model elements. The new version of KINEROS2 is linked to the ArcMap interface and allows users to view hydrographs of any of the reaches. A combination of the hydrographs and the maps could be extremely helpful for quickly identifying the reaches and planes that have large amounts of discharge.

Forecast KINEROS2 discharge using the HRM and GSM

Using the forecast rainfall provides an opportunity to issue FF warning relying on the modelling Q. The merit of the model was presented by the fitness of the simulated Q with the observed Q and the agreement between using Sat-P and the GSM and HRM rainfalls (Figure 10). However, some false alarms (marked by the circles) and overestimates at approximately 6 am on 26th June were found.

DISCUSSION

In performing FF prediction, we face great challenges and uncertainties concerning the input data and model structure
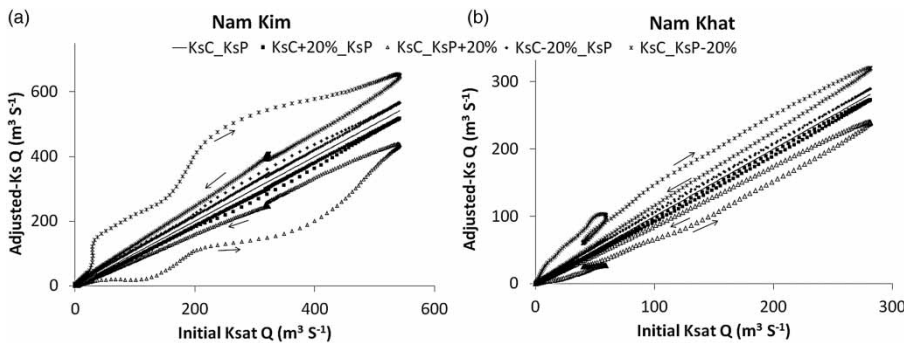
Figure 8 │ Effects of Ksat on the discharge simulated for the R23[rd] event (KsC and KsP refer to the channel and plane Ksat).

Table 4 │ Comparing the simulated discharge using the Sat-P and Rad-P for the R23[rd] event

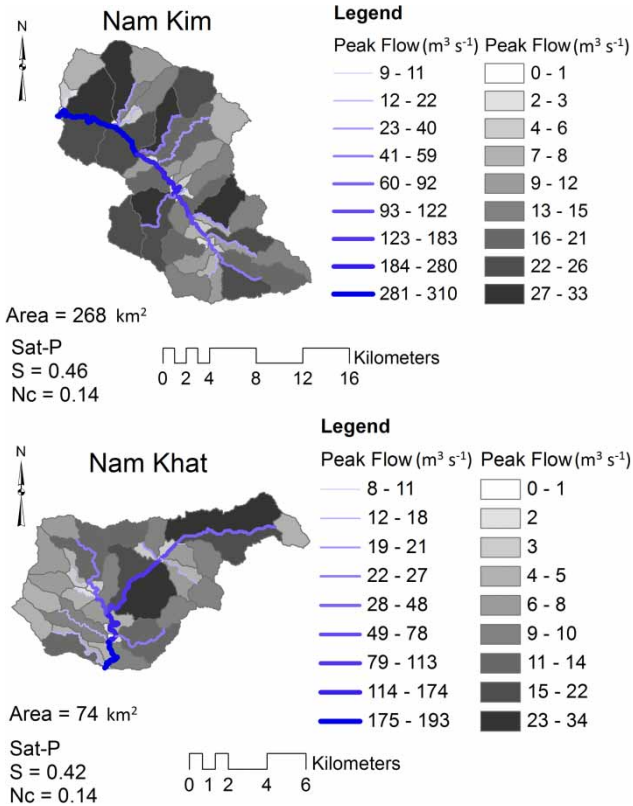| Parameters/Watersheds	Peak discharge (m³ s⁻¹)			Lags (hour)			Accumulative rainfall (mm)	
	Sat-P	Rad-P	Observed	Sat-P	Rad-P	Soil moisture (%)	Sat-P	Rad-P
NAM KIM	314.3	189.2	306.2	4.4	5.13	46	144.4	133.3
NAM KHAT	191.5	108.7	–	1.67	2.02	42	135.5	113.1

Figure 9 | Modelled stream and overland flow using KINEROS2.

(Montz & Gruntfest 2002). Although it is difficult to overcome these obstacles (Beven 2001), it is certainly not impossible. Many previous studies have failed to predict the stream runoff due to insufficient θ condition information (Ntelekos et al. 2006; Javelle et al. 2010; Marchi et al. 2010). Hence, the result of the certified BEACH model might play an important role to address this issue. In addition, all other inputs used for this study, such as the DEM, soil map, or LULC, were produced following the national norms or evaluated using a thorough accuracy assessment.

Concerning the model structure and parameter evaluations, all models were calibrated and validated. In particular, KINEROS2 was tested with several rainfall inputs; such testing had not been performed in many other works. This difference gives us opportunities to compare and contrast the outcomes. Some similarities of using the Gau-P and Sat-P outputs were found, whereas the supervised output of Rad-P underestimating the observed data was found. However, we do not judge that the Rad-P is less accurate than the Sat-P. It might be a question of the old radar generation used in Vietnam. As FFs often occur a short time after rains (4–6 hours) (NWS 2002), a good FF warning system should provide timely information (Lin
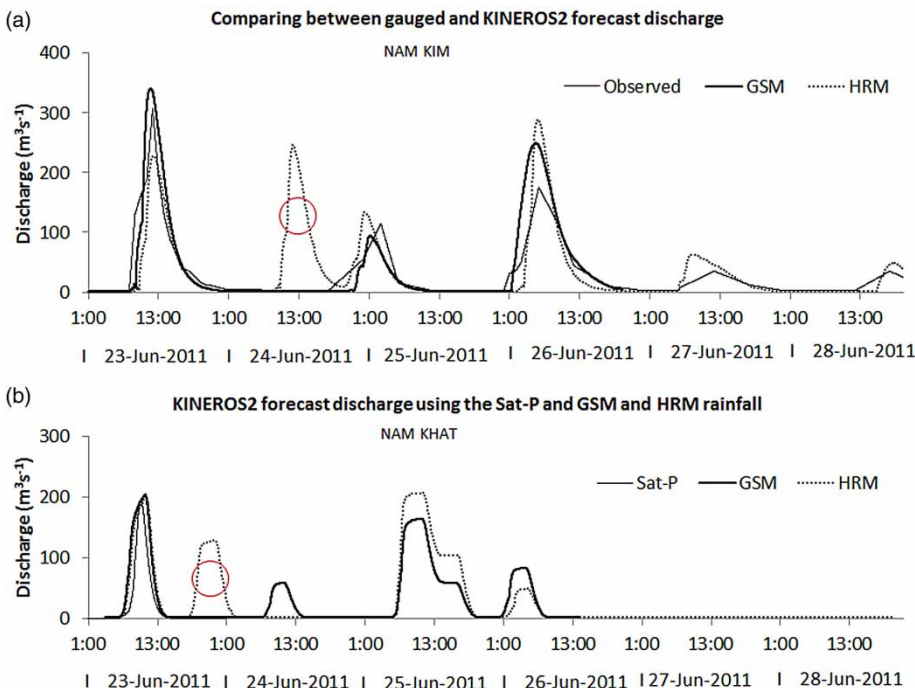

Figure 10 | Forecast Q_C using the GSM and HRM rainfall at the outlets of Nam Kim (a) and Nam Khat (b).

et al. 2002). This requirement is for the computational operation of models as well. KINEROS2 was validated using an Intel core™ i3, 2GB RAM computer, which only required approximately 20 seconds to run (at Nam Kim). This short run was one of the reasons for choosing this robust model. Only new updated FR is required for an up-coming forecast operation. Other parameters, such as the LULC, are recommended to be updated seasonally, and the soils and DEM are renewed in decades if significant changes are found.

Manual parameter calibration is a time-consuming implementation. Thus, the results of model parameter sensitivity tests might be significant for this work and for future studies as well. These study findings of substantial sensitivities of the Ksat, S and N to the model outputs are consistent with those of Memarian *et al.* (2013) and Martínez-Carreras *et al.* (2007). An important point is that this result of model calibration could be applied to ungauged 'neighbour' watersheds (Nam Khat for example) using a so-called 'regionalization approach' or similar methods already applied by Boughton & Chiew (2007), Makungo *et al.* (2010) and Servat & Dezetter (1993). Therefore, previously unresolved questions of flooding threshold determination for ungauged catchments might be answered. In addition, Carpenter *et al.* (1999) considered that the FF threshold is an essential part of FF warning systems. Unfortunately, the FF threshold varies naturally from watershed to watershed; as a result, traditional methods of evaluating the threshold using statistical reports were often not convincing (considering impacts of climate change) and inapplicable for ungauged catchments.

The uncertainties of a hydrological model's outputs are directly linked to rainfall estimations (Villarini *et al.* 2010). Currently, Adjei *et al.* (2015), Castro *et al.* (2014) and Xu *et al.* (2015) have introduced the newest rainfall estimation for tropical regions using satellite techniques. In addition, Finsen *et al.* (2014), Kang & Merwade (2014) and Wu *et al.* (2015) have made efforts to improve radar rainfall and to provide hydrological models with near or real-time data as well. Altogether, the above-described work gives more accurate rainfall availability for hydrological modellers. However, for operational FF prediction, very precise precipitation forecasts are needed at any given time. The GSM and HRM rainfalls were not expected to be the most suitable,

but were the only ones available at the time of this study in Vietnam. Because most parameters of the NWP models are highly nonlinear and naturally inconsistent (Majewski 2009; JMA 2013), uncertainties grow when the forecasted period expands further into the future. This might limit the average goal of the USA FF warning systems of 65% of correct alarms (Smith *et al.* 2005). As such, much work is required to improve the forecast of rainfall particularly with regard to extremes and the consequence of the prediction of FFs.

CONCLUSIONS

The θ_{ant} conditions were found to be extremely important for predicting the flooding magnitude and are therefore very helpful for providing FF guidance. However, unlike discharge and precipitation data, θ data are not routinely observed over a long period. Hence, the use of BEACH for E_a estimates is a promising approach. The Ksat was found to be the most sensitive parameter to determine the simulated Q_C. Although the variance of S and the Ksat had no impact on the time of Q's peak, changes in both parameters had significant effects on Q's volume. KINEROS2 represented a dynamic, robust hydrological model with the capability to simulate discharges (hydrographs) that fitted well to measured data using different rainfall sources. Therefore, we conclude KINEROS2 could be an appropriate model for the purpose of predicting the Q_C and thus for use in forecasts. The applications of the KINEROS2 model with the FR (from GSM and HRM) revealed the possibility to predict the time, magnitude and location of approaching FFs.

ACKNOWLEDGEMENTS

REFERENCES

Abderrezzak, K. E., Paquier, A. & Mignot, E. 2009 Modelling flash flood propagation in urban areas using a two-dimensional numerical model. *Nat. Hazards* **50** (3), 433–460. Doi:10.1007/s11069-008-9300-0.

Adjei, K. A., Ren, L. L., Appiah-Adjei, E. K. & Odai, S. N. 2015 Application of satellite-derived rainfall for hydrological modelling in the data-scarce Black Volta trans-boundary basin. *Hydrol. Res.*, **46** (5), 777–791.

Alfieri, L., Thielen, J. & Pappenberger, F. 2012 Ensemble hydro-meteorological simulation for flash flood early detection in southern Switzerland. *J. Hydrol.* **424**, 143–153. Doi:10.1016/j.jhydrol.2011.12.038.

Amengual, A., Romero, R., Gomez, M., Martin, A. & Alonso, S. 2007 A hydrometeorological modeling study of a flash-flood event over Catalonia, Spain. *J. Hydrometeorol.* **8** (3), 282–303. Doi:10.1175/Jhm577.1.

Ashley, S. T. & Ashley, W. S. 2008 Flood fatalities in the United States. *J. Appl. Meteor. Climatol.* **47**, 806–818.

Beven, K. 2001 How far can we go in distributed hydrological modelling? *Hydrol. Earth Syst. Sci.* **5** (1), 1–12.

Bloschl, G., Reszler, C. & Komma, J. 2008 A spatially distributed flash flood forecasting model. *Environ. Modell. Softw.* **23** (4), 464–478.

Boughton, W. & Chiew, F. 2007 Estimating runoff in ungauged catchments from rainfall, PET and the AWBM model. *Environ. Modell. Softw.* **22** (4), 476–487.

Brauer, C. C., Teuling, A. J., Overeem, A., van der Velde, Y., Hazenberg, P., Warmerdam, P. M. M. & Uijlenhoet, R. 2011 Anatomy of extraordinary rainfall and flash flood in a Dutch lowland catchment. *Hydrol. Earth Syst. Sci.* **15**, 1991–2005. Doi:10.5194/hess-15-1991-2011.

Carpenter, T. M., Sperfslage, J. A., Georgakakos, K. P., Sweeney, T. & Fread, D. L. 1999 National threshold runoff estimation utilizing GIS in support of operational flash flood warning systems. *J. Hydrol.* **224** (1–2), 21–44. Doi:.10.1016/s0022-1694(99)00115-8.

Castro, L. M., Salas, M. & Fernández, B. 2014 Evaluation of TRMM Multi-satellite precipitation analysis (TMPA) in a mountainous region of the central Andes range with a Mediterranean climate. *Hydrol. Res.* **46** (1), 89–105. Doi:10.2166/nh.2013.096.

Creutin, J. D., Borga, M., Gruntfest, E., Lutoff, C., Zoccatelli, D. & Ruin, I. 2013 A space and time framework for analyzing human anticipation of flash floods. *J. Hydrol.* **482**, 14–24.

El-Hames, A. S. & Richards, K. S. 1998 An integrated, physically based model for arid region flash flood prediction capable of simulating dynamic transmission loss. *Hydrol. Process.* **12** (8), 1219–1232.

Estupina-Borrell, V., Dartus, D. & Ababou, R. 2006 Flash flood modeling with the MARINE hydrological distributed model. *Hydrol. Earth Syst. Sci.* **3**, 3397–3438.

Finsen, F., Milzow, C., Smith, R., Berry, P. & Bauer-Gottwein, P. 2014 Using radar altimetry to update a large-scale hydrological model of the Brahmaputra river basin. *Hydrol. Res.* **45** (1), 143–164.

Garcia-Pintado, J., Barbera, G. G., Erena, M. & Castillo, V. M. 2009 Calibration of structure in a distributed forecasting model for a semiarid flash flood: Dynamic surface storage and channel roughness. *J. Hydrol.* **377** (1–2), 165–184.

Gupta, H. 2006 Final Report for COMET proposal entitled Development of a site-specific flash flood forecasting model for the Western Region. University of Arizona, Tucson, AZ, USA. http://www.comet.ucar.edu/outreach/abstract_final/0344674_AZ.pdf (accessed 20 November 2014).

Janal, P. & Stary, M. 2012 Fuzzy model used for the prediction of a state of emergency for a river basin in the case of a flash flood – Part 2. *J. Hydrol. Hydromech.* **60** (3), 162–173.

Javelle, P., Fouchier, C., Arnaud, P. & Lavabre, J. 2010 Flash flood warning at ungauged locations using radar rainfall and antecedent soil moisture estimations. *J. Hydrol.* **394** (1–2), 267–274.

JMA 2013 Outline of the Operational Numerical Weather Prediction at the Japan Meteorological Agency. Appendix to WMO Technical Progress Report on the Global Data-processing and Forecasting System (GDPFS) and Numerical Weather Prediction (NWP) Research. http://www.jma.go.jp/jma/jma-eng/jma-center/nwp/outline2013-nwp/pdf/outline2013_all.pdf (accessed 1 September 2014).

Kang, K. & Merwade, V. 2014 The effect of spatially uniform and non-uniform precipitation bias correction methods on improving NEXRAD rainfall accuracy for distributed hydrologic modeling. *Hydrol. Res.* **45** (1), 23–42.

Khavich, V. & Benzvi, A. 1995 Flash-flood forecasting-model for the Ayalon Stream, Israel. *Hydrol. Sci. J.* **40** (5), 599–613.

Kousky, C. & Walls, M. 2014 Floodplain conservation as a flood mitigation strategy: Examining costs and benefits. *Ecol. Econ.* **104**, 119–128.

Krishnamurti, T. N., Bedi, H. S., Hardiker, V. M. & Ramaswamy, L. 2006 *An Introduction to Global Spectral Modeling*. 2nd Revised and Enlarged Edition, Springer, Atmospheric and Oceanographic Sciences Library.

Li, L. & Xu, C.-Y. 2014 The comparison of sensitivity analysis of hydrological uncertainty estimates by GLUE and Bayesian method under the impact of precipitation errors. *Stoch. Env. Res. Risk. A.* **28** (3), 491–504.

Li, L., Xia, J., Xu, C.-Y. & Singh, V. P. 2010 Evaluation of the subjective factors of the GLUE method and comparison with the formal Bayesian method in uncertainty assessment of hydrological models. *J. Hydrol.* **390**, 210–221.

Li, L., Xu, C.-Y. & Engeland, K. 2013 Development and comparison in uncertainty assessment based Bayesian modularization method in hydrological modeling. *J. Hydrol.* **486**, 384–394.

Lin, C. A., Wen, L., Beland, M. & Chaumont, D. 2002 A coupled atmospheric-hydrological modeling study of the 1996 Ha!

Ha! River basin flash flood in Quebec, Canada. *Geophys. Res. Lett.* **29** (2), 13-1–13-4.

Looper, J. P. & Vieux, B. E. 2012 An assessment of distributed flash flood forecasting accuracy using radar and rain gauge input for a physics-based distributed hydrologic model. *J. Hydrol.* **412**, 114–132.

Majewski, D. 2009 HRM – User's Guide for the HRM with the SSO scheme (Vrs. 2.5 and higher). Deutscher Wetterdienst, Press and Public Relations, Offenbach, Germany. http://www.dwd. de/SharedDocs/downloads/DE/modelldokumentationen/n wv/hrm/HRM_users_guide.pdf?__blob=publication File&v=2 (accessed 4 November 2014).

Makungo, R., Odiyo, J. O., Ndiritu, J. G. & Mwaka, B. 2010 Rainfall– runoff modelling approach for ungauged catchments: A case study of Nzhelele River sub-quaternary catchment. *Phys. Chem. Earth, Parts A/B/C*, **35** (13–14), 596–607.

Marchi, L., Borga, M., Preciso, E. & Gaume, E. 2010 Characterisation of selected extreme flash floods in Europe and implications for flood risk management. *J. Hydrol.* **394** (1–2), 118–133.

Marshall, J. S., Langille, R. C. & Palmer, W. M. K. 1947 Measurement of rainfall by radar. *J. Meteorol.* **4** (6), 186–192.

Martínez-Carreras, N., Soler, M., Hernández, E. & Gallart, F. 2007 Simulating badland erosion with KINEROS2 in a small Mediterranean mountain basin (Vallcebre, Eastern Pyrenees). *Catena* **71** (1), 145–154.

Memarian, H., Balasundram, S. K., Talib, J. B., Teh Boon Sung, C., Mohd Sood, A. & Abbaspour, K. C. 2013 KINEROS2 application for land use/cover change impact analysis at the Hulu Langat Basin, Malaysia. *Water and Environ. J.* **27** (4), 549–560.

Montz, B. E. & Gruntfest, E. 2002 Flash flood mitigation: recommendations for research and applications. *Global Environ. Change B Environ. Hazard.* **4** (1), 15–22.

Morin, E., Jacoby, Y., Navon, S. & Bet-Halachmi, E. 2009 Towards flash-flood prediction in the dry Dead Sea region utilizing radar rainfall information. *Adv. Water Resour.* **32** (7), 1066– 1076.

NCHMF 2011 Vietnam National Centre for Hydro-Meteorological Forecasting. http://www.nchmf.gov.vn/web/vi-VN/71/29/ 45/Default.aspx (accessed 7 March 2014).

Neitsch, S. L., Arnold, J. G., Kiniry, J. R. & Williams, J. R. 2009 Soil and Water Assessment Tool Theoretical Documentation, Version 2009. Texas Water Resources Institute Technical Report No. 406.

Ntelekos, A. A., Georgakakos, K. P. & Krajewski, W. F. 2006 On the uncertainties of flash flood guidance: Toward probabilistic forecasting of flash floods. *J. Hydrometeorol.* **7** (5), 896–915.

NWS 2002 Advanced hydrologic prediction services – Concept of services and operations. Report U.S. Department of Commerce – NOAA – NWS.

Quintero, F., Sempere-Torres, D., Berenguer, M. & Baltas, E. 2012 A scenario-incorporating analysis of the propagation of uncertainty to flash flood simulations. *J. Hydrol.* **460**, 90–102.

Reed, S., Schaake, J. & Zhang, Z. Y. 2007 A distributed hydrologic model and threshold frequency-based method for flash flood forecasting at ungauged locations. *J. Hydrol.* **337** (3–4), 402– 420.

Ruin, I., Creutin, J. D., Anquetin, S. & Lutoff, C. 2008 Human exposure to flash floods – Relation between flood parameters and human vulnerability during a storm of September 2002 in Southern France. *J. Hydrol.* **361** (1–2), 199–213.

Sahoo, G. B., Ray, C. & De Carlo, E. H. 2006 Use of neural network to predict flash flood and attendant water qualities of a mountainous stream on Oahu, Hawaii. *J. Hydrol.* **327** (3–4), 525–538.

Semmens, D. J., Goodrich, D. C., Unkrich, C. L., Smith, R. E., Woolhiser, D. A. & Miller, S. N. 2008 KINEROS2 And the AGWA modeling framework. In: H. S. Wheater, S. Sorooshian & K. D. Sharma (eds). *Hydrological Modelling in Arid and Semi-arid Areas*. Cambridge University Press, Cambridge, pp. 41–48.

Seo, D., Lakhankar, T., Mejia, J., Cosgrove, B. & Khanbilvardi, R. 2012 Evaluation of Operational National Weather Service Gridded Flash Flood Guidance over the Arkansas Red River Basin. *J. Am. Water Resour. Assoc. (JAWRA)* **49** (6), 1296– 1307.

Servat, E. & Dezetter, A. 1993 Rainfall-runoff modelling and water resources assessment in northwestern Ivory Coast. Tentative extension to ungauged catchments. *J. Hydrol.* **148** (1–4), 231–248.

Sheikh, V., Visser, S. & Stroosnijder, L. 2009 A simple model to predict soil moisture: Bridging Event and Continuous Hydrological (BEACH) modelling. *Environ. Modell. Softw.* **24** (4), 542–556.

Smith, R. E., Goodrich, D. C., Woolhiser, D. A. & Unkrich, C. L. 1995 KINEROS – A kinematic runoff and erosion model. In: V. P. Singh (ed.). *Computer Models of Watershed Hydrology*. Water Resources Publications, Highlands Ranch, CO, 1130 pp.

Smith, P. L., Barros, A., Chandrasekar, V., Forbes, G., Gruntfest, E., Krajewski, W. & Galinis, E. 2005 *Flash Flood Forecasting over Complex Terrain with an Assessment of the Sulphur Mountain NEXRAD in Southern California*. The National Academies Press, Washington, DC. www.nap.edu.

Thiessen, A. H. 1911 Precipitation averages for large areas. *Monthly Weather Rev.* **39** (7), 1082–1089.

Versini, P. A. 2012 Use of radar rainfall estimates and forecasts to prevent flash flood in real time by using a road inundation warning system. *J. Hydrol.* **416**, 157–170.

Villarini, G., Krajewski, W. F., Ntelekos, A. A., Georgakakos, K. P. & Smith, J. A. 2010 Towards probabilistic forecasting of flash floods: The combined effects of uncertainty in radar-rainfall and flash flood guidance. *J. Hydrol.* **394** (1–2), 275–284.

Vincendon, B., Ducrocq, V., Dierer, S., Kotroni, V., Le Lay, M., Milelli, M. & Steiner, P. 2009 Flash flood forecasting within the PREVIEW project: value of high-resolution hydrometeorological coupled forecast. *Meteor. Atmos. Phys.* **103** (1–4), 115–125.

Volkmann, T. H. M., Lyon, S. W., Gupta, H. V. & Troch, P. A. 2010 Multicriteria design of rain gauge networks for flash flood prediction in semiarid catchments with complex terrain. *Water Resour. Res.* **46**, W11554.

Woolhiser, D. A., Smith, R. E. & Goodrich, D. C. 1990 *KINEROS, A Kinematic Runoff and Erosion Model. Documentation and User Manual*. ARS-77. USDA, ARS, Washington, DC.

Wu, S.-J., Lien, H.-C., Hsu, C.-T., Chang, C.-H. & Shen, J.-C. 2015 Modeling probabilistic radar rainfall estimation at ungauged locations based on spatiotemporal errors which correspond to gauged data. *Hydrol. Res.* **46** (1), 39–59.

Xu, H., Xu, C.-Y., Sælthun, N.-R., Zhou, B. & Xu, Y. P. 2015 Evaluation of reanalysis and satellite-based precipitation datasets in driving hydrological models in a humid region of Southern China. *Stoch. Environ. Res. Risk Assess.* **29** (8), 2003–2020.

Younis, J., Anquetin, S. & Thielen, J. 2008 The benefit of high-resolution operational weather forecasts for flash flood warning. *Hydrol. Earth Syst. Sci.* **12**, 1039–1051.